

Curvature calculations for the level-set method

Karl Yngve Lervåg and Åsmund Ervik

Abstract The present work illustrates a difficulty with the level-set method to accurately capture the curvature of interfaces in regions that are of equal distance to two or more interfaces. Such regions are characterized by kinks in the level-set function where the derivative is discontinuous. Thus the standard discretization scheme is not suitable. Three discretization schemes are outlined that are shown to perform better than the standard discretization on two selected test cases.

1 Introduction

This article addresses the calculation of interface curvature with the level-set method. In the level-set method, the normal vector and the curvature of an interface can be calculated directly from the level-set function. These calculations are usually done with standard finite-difference methods, typically the second-order central difference scheme (CD-2) [10, 12, 4].

A problem with these calculations may arise when the level-set function is defined to be a signed-distance function. The signed-distance function is in general not smooth, as can be seen in Figure 1. Here the derivative of the level-set function will be discontinuous at the regions that are of equal distance to more than one interface. When two droplets as in Figure 1 are in near contact, such discontinuities, or kinks, may lead to significant errors when calculating the interface geometries with standard finite difference methods.

Karl Yngve Lervåg, e-mail: karl.yngve@lervag.net
 Norwegian University of Science and Technology, Department of Energy and Process Engineering,
 Kolbjørn Hejes veg 2, NO-7491 Trondheim, Norway.

Åsmund Ervik, e-mail: aaervik@gmail.com
 SINTEF Energy Research, Sem Sælands veg 11, NO-7465 Trondheim, Norway.
 Norwegian University of Science and Technology, Department of Physics, Høgskoleringen 5, NO-7491 Trondheim, Norway.

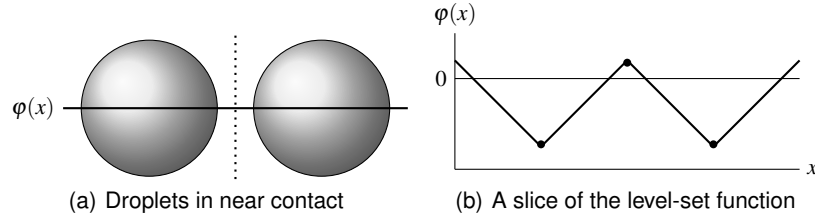


Fig. 1 (a) Two droplets in near contact. The dotted line marks a region where the derivative of the level-set function is not defined. (b) A one-dimensional slice of the level-set function $\phi(x)$. The dots mark points where the derivative of $\phi(x)$ is not defined.

2 Governing equations

2.1 Navier-Stokes equations for two-phase flow

Consider a domain $\Omega = \Omega^+ \cup \Omega^-$, where Ω^+ and Ω^- denote regions occupied by two respective phases, divided by an interface $\Gamma = \delta\Omega^+ \cap \delta\Omega^-$. The governing equations for incompressible and immiscible two-phase flow in the domain Ω with an interface force on the interface Γ are

$$\nabla \cdot \mathbf{u} = 0, \quad (1)$$

$$\rho \left(\frac{\partial \mathbf{u}}{\partial t} + \mathbf{u} \cdot \nabla \mathbf{u} \right) = -\nabla p + \nabla \cdot (\mu \nabla \mathbf{u}) + \rho \mathbf{f}_b + \int_{\Gamma} \sigma \kappa \mathbf{n} \delta(\mathbf{x} - \mathbf{x}_I(s)) ds. \quad (2)$$

Here \mathbf{u} is the velocity vector, p is the pressure, \mathbf{f}_b is the specific body force, σ is the coefficient of surface tension, κ is the curvature, \mathbf{n} is the normal unit vector which points into Ω^+ , δ is the Dirac delta function, $\mathbf{x}_I(s)$ is a parametrization of the interface, ρ is the density and μ is the viscosity.

It is assumed that the density and viscosity are constant in each phase, but may be discontinuous across the interface. The jump conditions across the interface are

$$[[\mathbf{u}]] = 0, \quad (3)$$

$$[[p]] = 2[[\mu]] \mathbf{n} \cdot \nabla \mathbf{u} \cdot \mathbf{n} + \sigma \kappa, \quad (4)$$

$$[[\mu \nabla \mathbf{u}]] = [[\mu]] \left((\mathbf{n} \cdot \nabla \mathbf{u} \cdot \mathbf{n}) \mathbf{n} \mathbf{n} + (\mathbf{n} \cdot \nabla \mathbf{u} \cdot \mathbf{t}) \mathbf{n} \mathbf{t} + (\mathbf{n} \cdot \nabla \mathbf{u} \cdot \mathbf{t}) \mathbf{t} \mathbf{n} + (\mathbf{t} \cdot \nabla \mathbf{u} \cdot \mathbf{t}) \mathbf{t} \mathbf{t} \right), \quad (5)$$

where \mathbf{t} is the tangent vector along the interface and $[[\cdot]]$ denotes the jump across an interface, that is $[[\mu]] \equiv \mu^+ - \mu^-$. Note that $\nabla \mathbf{u}$ and (e.g.) $\mathbf{n} \mathbf{t}$ are rank-2 tensors. See [4, 3] for more details and a derivation of the interface conditions.

2.2 Level-set method

The interface is captured with the zero level set of the level-set function $\varphi(\mathbf{x}, t)$, which is prescribed as a signed-distance function. It is updated by solving an advection equation for φ ,

$$\frac{\partial \varphi}{\partial t} + \hat{\mathbf{u}} \cdot \nabla \varphi = 0, \quad (6)$$

where $\hat{\mathbf{u}}$ is the velocity at the interface, extended to the entire domain by solving

$$\frac{\partial \hat{\mathbf{u}}}{\partial \tau} + S(\varphi) \mathbf{n} \cdot \nabla \hat{\mathbf{u}} = 0, \quad \hat{\mathbf{u}}_{\tau=0} = \mathbf{u}, \quad (7)$$

to steady state, cf. [15]. Here τ is a pseudo-time and $S(\varphi) = \varphi / (\varphi^2 + 2\Delta x^2)^{1/2}$ is a smeared sign function which is equal to zero at the interface.

When (6) is solved numerically, the level-set function loses its signed-distance property due to numerical dissipation. The level-set function is therefore reinitialized regularly by solving

$$\begin{aligned} \frac{\partial \varphi}{\partial \tau} + S(\varphi_0)(|\nabla \varphi| - 1) &= 0, \\ \varphi(\mathbf{x}, 0) &= \varphi_0(\mathbf{x}), \end{aligned} \quad (8)$$

to steady state as proposed in [13], where φ_0 is the level-set function that needs to be reinitialized.

Normal vectors and curvatures can be readily calculated from the level-set function as

$$\mathbf{n} = \frac{\nabla \varphi}{|\nabla \varphi|} \quad \text{and} \quad \kappa = \nabla \cdot \left(\frac{\nabla \varphi}{|\nabla \varphi|} \right). \quad (9)$$

3 Numerical methods

The Navier-Stokes equations (1) and (2) are solved using a projection method on a staggered grid as described in [3, Chapter 5.1.1]. The spatial terms are discretized with CD-2, except for the convective terms which are discretized by a fifth-order WENO scheme. A third-order strong stability-preserving Runge-Kutta (SSP RK) method is used for the momentum equation (2), and a second-order SSP-RK method is used for the level-set equations (6) to (8) [2].

The interface conditions are treated in a sharp fashion with the Ghost-Fluid Method (GFM), which incorporates the discontinuities into the discretization stencils by altering the stencils close to the interfaces, cf. [1, 4, 6]. When using the GFM, the curvature is linearly interpolated from the grid points to the interface before it is used in the discretization stencils for the flow equations unless otherwise stated.

4 Curvature discretizations

The normal vector and the curvature (9) are typically discretized with the CD-2 at the grid points, cf. [4, 12, 14]. A problem with this is that CD-2 will not converge across kinks, and it may therefore introduce potentially large errors. The errors in the curvature will lead to erroneous pressure jumps at the interfaces, and the errors in the normal vector affect both the discretized interface conditions and the extrapolated velocity (7) which is used in the advection equation (6).

A direction difference scheme is presented in [7] which uses a combination of one-sided and central difference schemes to ensure that the differences never cross kinks. The same scheme is used in the present work to calculate the normal vector. The idea is choose which difference scheme to use based on the values of a quality function,

$$Q(\mathbf{x}) = |1 - |\nabla\phi(\mathbf{x})||. \quad (10)$$

The quality function is itself calculated with central differences. It effectively detects the regions where the level-set function differs from the signed-distance function. Let $Q_{i,j} = Q(\mathbf{x}_{i,j})$ and $\eta > 0$, then $Q_{i,j} > \eta$ can be used to detect kinks. The parameter η is tuned such that the quality function will detect all the kinks. The value $\eta = 0.1$ is used in the present work.

In the following, three different improved discretization schemes for the curvature are outlined. Note that the first two schemes use the quality function to detect when the improved schemes should be used in favor of CD-2. Also note that the curvature is only calculated at grid points in a narrow band along the interface. At the points where it is not calculated, it is set to zero.

Macklin and Lowengrub's method (MLM) was presented in [8, 9]. With this method, the interface is parametrized with a second-order least-squares polynomial. The curvature is then calculated directly from the parametrization at the desired position on the interface.

To enable easy comparison with the other methods, the estimated curvature values are extrapolated from the interface to the adjacent grid points.

Lervåg's method (LM) was presented in [5] and is based on MLM, specifically [8]. The curve parametrization is used to create a local level-set function from which the curvature is calculated on the grid points using CD-2.

The main difference from MLM is that the curvature is calculated at the grid nodes and then interpolated to the interface afterwards. This is argued as a slight simplification of MLM, although an important consequence is that it becomes more important to have an accurate representation of the interface. Instead of using a least-squares parametrization, LM uses monotone cubic Hermite splines.

Salac and Lu's method (SLM) was presented in [11] and is a different approach than MLM and LM. Consider the 2D case of two circles in near contact, see Figure (2). SLM reconstructs two independent level-set functions ϕ_1 and ϕ_2 for the two circles. The reconstructed functions are then used to calculate the curvature. Since the two reconstructed cones have no kinks, the curvature can be calculated with CD-2. For points close to both circles, a weighted average of the curvature from ϕ_1 and

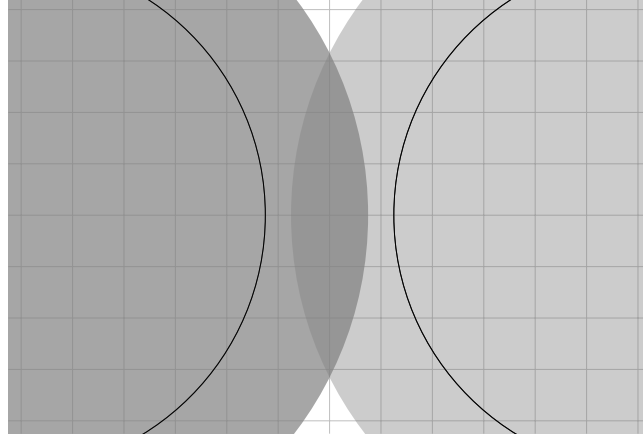


Fig. 2 Simple sketch of how SLM works. The two circles are represented by separate level-set functions.

from ϕ_2 is stored. For points close to only one circle, the appropriate curvature is stored. The weighted average is $\kappa = (\kappa_1 \phi_2 + \kappa_2 \phi_1) / (\phi_1 + \phi_2)$, where the subscripts refer to values calculated on the reconstructed level-set functions. This weighting will prefer κ_1 when closest to circle 1, and vice versa.

5 Comparison of the discretization schemes

5.1 A static disc above a rectangle

Consider a disc of radius r positioned at a distance h above a rectangle, see Figure 3(a). In this case, only the level-set function and the geometrical quantities are considered. None of the governing equations (1), (2) and (6) to (8) are solved.

The parameters used for this case are $r = 0.25$ m and $h = \Delta x$. The domain is $1.5 \text{ m} \times 1.5 \text{ m}$, and the rectangle height is 0.75 m. The grid size is 101×101 .

Figure 4 shows a comparison of the calculated curvatures. The figure shows that CD-2 leads to large errors in the calculated curvatures in the areas that are close to two interfaces. In particular note that the sign of the curvature becomes wrong. The analytic curvature for this case is $\kappa = -1/r = -4$, and the curvature spikes seen for the standard discretization is of the order of $|\kappa| \sim \frac{1}{\Delta x} \simeq 67.3$. All of the improved methods give much better estimates of the curvature, as expected.

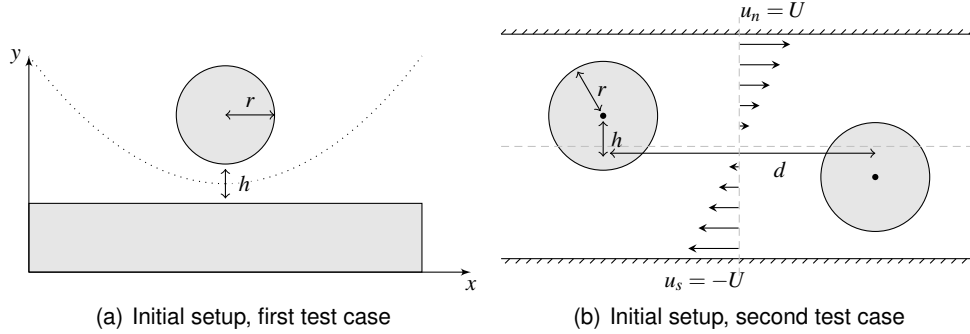


Fig. 3 Initial setup for the circle and rectangle test, (a), and for the drop collision in shear flow test, (b). In (a), the dotted line depicts the kink location, and there is no flow. In (b) the flow is indicated by the velocity profile.

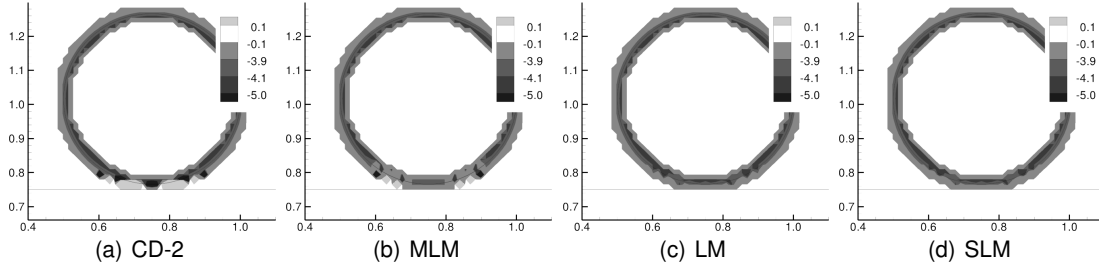


Fig. 4 A comparison of curvature calculations between standard discretization and the improved method. The standard discretization leads to large errors in the curvatures in areas that are close to two interfaces.

5.2 Drop collision in shear flow

Now consider two drops in a shear flow as depicted in Figure 3(b). Both drops have radius r and are initially placed a distance $d = 5r$ apart in the shear flow, where the flow velocity changes linearly from $u_s = -U < 0$ at the bottom wall to $u_n = U$ at the top wall. The computational domain is $12r \times 8r$, and the grid size is 241×161 . The density and viscosity differences of the two phases are zero.

The shear flow is defined by the Reynolds number and the Capillary number,

$$Re = \frac{\rho U r}{\mu} \quad \text{and} \quad Ca = \frac{\mu U}{\sigma}. \quad (11)$$

The following results were obtained with $r = 0.5$ m, $h = 0.84r = 0.42$ m, $Re = 10$ and $Ca = 0.025$.

Figure 5 shows a comparison of the interface evolution and the curvature between the different discretization schemes. The first column shows the results with the

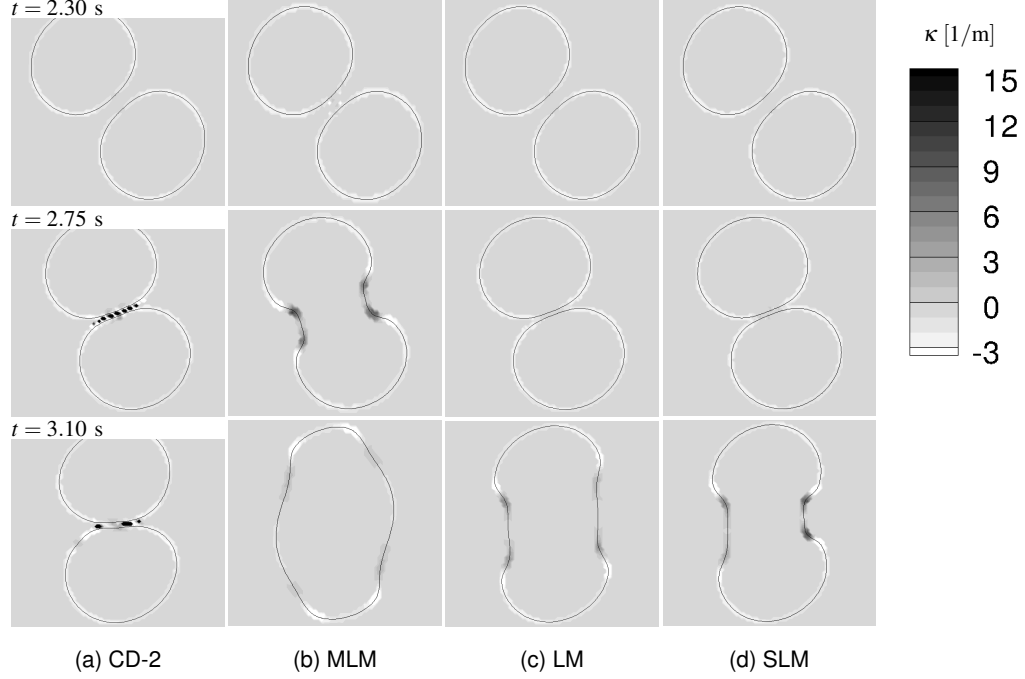


Fig. 5 A comparison between the different discretization schemes of the interface evolution and the curvature κ of drop collision in shear flow.

CD-2. The next three columns show the results with the three improved schemes respectively. The kinks between the drops lead to curvature spikes with CD-2, whereas the improved discretizations calculate the curvature along the kink in a much more reliable manner. LM and SLM give very similar results. This is most likely due to the fact that both these methods calculate the curvature at the grid points and then interpolate, resulting in very similar algorithms as long as the curvature calculations are accurate. MLM on the other hand removes the interpolation step and calculates the curvature directly on the interface. Note that the difference is mainly that the MLM results in slightly earlier coalescence in the given case.

The curvature spikes in obtained with CD-2 are seen to prevent coalescence. This is due to the effect they have on the pressure field as displayed in Figure 6. Here it is shown that the errors in the curvature with CD-2 lead to an erroneous pressure field between the drops. The distortion of the pressure in the thin-film region leads to a flow into the film region that suppresses coalescence. The corresponding result with LM shows that when the pressure is not distorted, it leads to a flow directed out of the thin-film region.

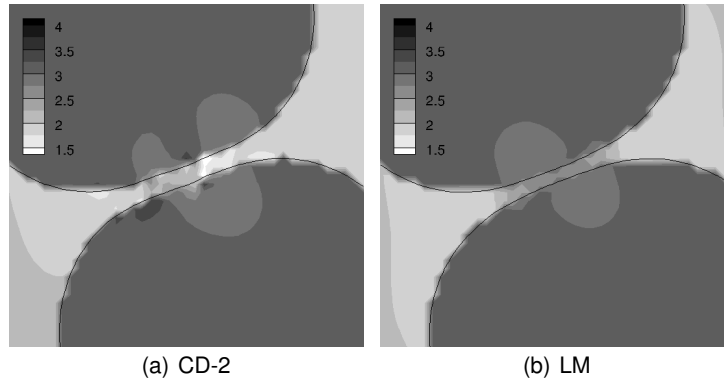


Fig. 6 Comparison of the pressure field in the thin film between the droplets at $t = 2.75$ s. The contour legends indicate the pressure in Pa.

6 Conclusions

Three discretization schemes have been implemented to accurately calculate the curvature in regions close to kinks in the level-set function. It has been demonstrated in two test cases that the standard second-order central difference scheme (CD-2) leads to relatively severe errors across the kinks. Macklin and Lowengrub's method (MLM), Lervåg's method (LM), and Salac and Lu's method (SLM) all give better results. In the second test case where two droplets are put in a shear flow, CD-2 gives a qualitatively different result than all the three improved schemes due to an erroneous pressure field in the thin film region.

Acknowledgements

The authors acknowledge Bernhard Müller (Norwegian University of Science and Technology) and Svend Tollak Munkejord (SINTEF Energy Research) for valuable feedback on the manuscript.

This work was financed through the Enabling Low-Emission LNG Systems project, and the authors acknowledge the contributions of GDF SUEZ, Statoil and the Petromaks programme of the Research Council of Norway (193062/S60).

References

1. Fedkiw, R.P., Aslam, T., Merriman, B., Osher, S.: A non-oscillatory Eulerian approach to interfaces in multimaterial flows (the ghost fluid method). *Journal of Computational Physics*

- 152**(2), 457–492 (1999). DOI 10.1006/jcph.1999.6236
2. Gottlieb, S., Shu, C.W., Tadmor, E.: Strong stability-preserving high-order time discretization methods. *SIAM Review* **43**, 89–112 (2001)
3. Hansen, E.B.: Numerical simulation of droplet dynamics in the presence of an electric field. Doctoral thesis, Norwegian University of Science and Technology, Department of Energy and Process Engineering, Trondheim (2005). ISBN 82-471-7318-2
4. Kang, M., Fedkiw, R.P., Liu, X.D.: A boundary condition capturing method for multiphase incompressible flow. *Journal of Scientific Computing* **15**(3), 323–360 (2000)
5. Lervåg, K.Y.: Calculation of interface curvature with the level-set method. In: Sixth National Conference on Computational Mechanics MekIT'11 (Trondheim, Norway) (23-24 May 2011)
6. Liu, X.D., Fedkiw, R.P., Kang, M.: A boundary condition capturing method for Poisson's equation on irregular domains. *Journal of Computational Physics* **160**, 151–178 (2000)
7. Macklin, P., Lowengrub, J.: Evolving interfaces via gradients of geometry-dependent interior Poisson problems: Application to tumor growth. *Journal of Computational Physics* **203**, 191–220 (2005)
8. Macklin, P., Lowengrub, J.: An improved geometry-aware curvature discretization for level set methods: Application to tumor growth. *Journal of Computational Physics* **215**, 392–401 (2006)
9. Macklin, P., Lowengrub, J.S.: A new ghost cell/level set method for moving boundary problems: Application to tumor growth. *Journal of Scientific Computing* **35**, 266–299 (2008)
10. Osher, S., Sethian, J.A.: Fronts propagating with curvature dependent speed: Algorithms based on Hamilton-Jacobi formulations. *Journal of Computational Physics* **79**, 12–49 (1988)
11. Salac, D., Lu, W.: A local semi-implicit level-set method for interface motion. *Journal of Scientific Computing* **35**, 330–349 (2008)
12. Sethian, J.A., Smereka, P.: Level set methods for fluid interfaces. *Annual Review of Fluid Mechanics* **35**, 341–372 (2003)
13. Sussman, M., Smereka, P., Osher, S.: A level set approach for computing solutions to incompressible two-phase flow. *Journal of Computational Physics* **114**, 146–159 (1994)
14. Xu, J.J., Li, Z., Lowengrub, J., Zhao, H.K.: A level set method for interfacial flows with surfactants. *Journal of Computational Physics* **212**(2), 590–616 (2006)
15. Zhao, H.K., Chan, T., Merriman, B., Osher, S.: A variational level set approach to multiphase motion. *Journal of Computational Physics* **127**, 179–195 (1996)